Chinese Chemical Letters 34 (2023) 108304

Contents lists available at ScienceDirect

Chinese Chemical Letters

journal homepage: www.elsevier.com/locate/cclet

Hydrogen-bonding-driven self-assembly nonporous adaptive crystals for the separation of benzene from BTX and cyclohexane☆

Fei Zeng[a,*], Lin-Li Tang[a], Hui Yu[a], Fan-Ping Xu[a], Leyong Wang[b]

[a] *Department of Biology and Chemistry, Hunan University of Science and Engineering, Yongzhou 425199, China*
[b] *School of Chemistry and Chemical Engineering Nanjing University, Nanjing 210023, China*

A R T I C L E I N F O

Article history:
Received 26 December 2022
Revised 21 February 2023
Accepted 5 March 2023
Available online 11 March 2023

Keywords:
Benzene separation
Self-assembly
Hydrogen bonding
Supramolecular chemistry
Nonporous adaptive crystals

A B S T R A C T

Benzene is a volatile organic compound that can seriously harm human health, while it can serve as a precursor to produce chemicals of more complex structures in chemical industry. Capturing benzene using adsorbents is of great importance for human health, when the separation of hydrocarbons including benzene from crude oil was referred to as one of the "seven chemical separations to change the world". In this work, we reported the efficient and selective separation of benzene from BTX and cyclohexane by hydrogen bonding self-assembly nonporous adaptive crystals AdaOH for the first time under mild and user-friendly conditions. Separation of benzene and cyclohexane (v/v = 1:1) can be achieved by AdaOH with a purity of benzene up to 96.8%. Separation of BTX (v/v; benzene:toluene:*o*-xylene:*m*-xylene:*p*-xylene= 1:1:1:1:1) can be achieved by AdaOH with a purity of benzene increased from 20% to 82.9%. Our results suggest that separation of benzene using the activated AdaOH as a non-porous adaptive crystal for selectively and efficiently capturing benzene can solve the challenge in separation of benzene from other chemicals such as cyclohexane in chemical industry, and can be helpful for removal of benzene that is released from the vehicles to air. The advantages of commercially availability, easy preparation, high separation efficiency and selectivity for benzene might endow this material with enormous potential for practical uses in areas like petrochemical industry.

Gasoline [1], as a complex mixture of volatile and flammable hydrocarbons, contains about 21% BTX (benzene, toluene (Tol), and xylene (*o*X, *m*X, *p*X)). Because of the incomplete combustion of gasoline, the exhaust gases of vehicles containing a large amount of BTX are released to the air, causing environmental pollution [2]. As a member of BTX gases, benzene (PhH) is harmful to human health, and can cause various diseased [3,4]. With the increasing consumption of gasoline by a large number of vehicles, benzene-induced environmental pollution facing the world is becoming increasingly serious. Thus, it is very urgent to develop new technologies with environmental-friendly, recyclable, low cost and high selectivity to reduce the amount of benzene in exhaust gases of cars. Recently, using activated carbon as adsorbent to adsorption of benzene from automotive gasoline has become a hot topic in the field of material science [5–9]. Employing MOFs for the separation of industrially important hydrocarbon mixtures has also been experimentally investigated [10–19].

Although it can cause environmental pollution, benzene can serve as an important raw material to produce chemicals of more complex structures in chemical industry as well [20]. Cyclohexane (Cy), that is a feedstock for varnishes, resins and nylon fibers [21], is often produced by the hydrogenation of benzene. The difference of 0.6 K between the boiling points of PhH (353.25 K) and Cy (353.85 K) is almost negligible, and the azeotrope of PhH and Cy is easily formed. Because of these, the removal of unreacted PhH from the reactor's effluent stream to afford pure Cy is referred to as one of the most challenging tasks in the petrochemical industries [22]. Currently, methodologies of physical adsorption of hydrocarbons using macrocycle-based nonporous adaptive crystals (NACs) have showed better performances over those of traditional extractive and azeotropic distillations [23–37]. Several groups including our group have separately reported the separation of PhH and Cy using different synthetic macrocycle-based nonporous adaptive crystals (NACs) [38–42]. However, all of these progresses focused on the separation of PhH and Cy. The similarities of structure and electrostatic potential characteristics between PhH and BTX result in the great difficulty of removing PhH with a low concentration from BTX. To the best of our knowledge, the selective and efficient

☆ Dedication to Prof. Lixin Dai on the Occasion of His Centenary Birthday.

* Corresponding author.
E-mail address: zengfei@iccas.ac.cn (F. Zeng).

https://doi.org/10.1016/j.cclet.2023.108304
1001-8417/

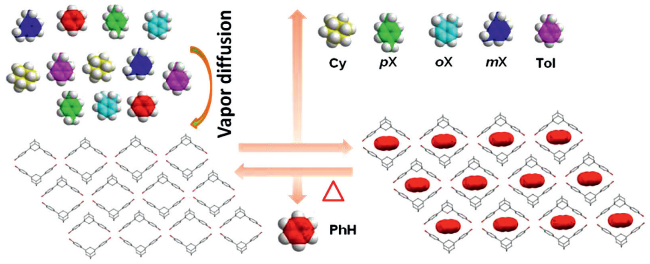

Fig. 1. Structural representation of the capture of PhH from a PhH/Cy mixture and BTX using AdaOH crystals.

capture of PhH from BTX by nonporous adaptive crystals were unexplored, although the Yoshizawa group [43] reported that a capsule structure can efficiently and selectively capture *o*-xylene over toluene, benzene, and cyclohexane. Given that separation of PhH from mixtures like BTX can provide benzene for the chemical industry and reduce the environmental pollution, a new material, that can efficiently separate PhH from mixtures such as BTX and that of PhH and Cy, is still challenging but greatly required.

Herein, as part of our research interests in the separation of hydrocarbons [44–46], we report the high unusual vapor adsorption behavior toward PhH over toluene, xylene, and Cy by commercially available 4,4'-(adamantane-1,3-diyl)diphenol (AdaOH) under room temperature and atmospheric pressure (Fig. 1). The AdaOH used as an adsorption material for PhH has the following advantages: (a) adsorption of PhH with high efficiency and selectivity. Separation of equimolar PhH and Cy can be achieved by AdaOH with a purity of PhH up to 96.8%. Separation of BTX (v/v; benzene:toluene:*o*-xylene:*m*-xylene:*p*-xylene = 1:1:1:1:1) can be achieved by AdaOH with a purity of PhH up to 82.9%; (b) easy prepared and commercially available; (c) reusability. After five cycles of adsorption and desorption, AdaOH was still able to selectively adsorb PhH from BTX and mixtures of PhH and Cy without losing performance; (d) AdaOH is a crystalline adsorbent, obtained by hydrogen bonding-driven self-assembly. This new discovery will open a new window for the development of new adsorption materials for PhH.

The activated AdaOH was first prepared according to the reported literature [47] and dried under vacuum at 150 °C for 6 h. The ^{1}H NMR spectrum shows no organic solvent signals, indicating the removal of the residual organic solvents. The thermogravimetric analysis (TGA) results also verified the complete removal of the residual organic solvents, in which no weight loss was observed for the activated solids below 200 °C (Fig. S1 in Supporting information). The powder X-ray diffraction analysis (PXRD) patterns of AdaOH showed sharp peaks, suggested that AdaOH maintained its crystallinity after losing the solvent (Fig. S2 in Supporting information). A N_2 sorption experiment at 77 K revealed the Brunauer–Emmett–Teller (BET) surface area of AdaOH was 4.47 m^2/g, suggested the nonporous character of AdaOH (Fig. S3 in Supporting information).

To test the adsorption behavior of activated AdaOH toward PhH and Cy, single component solid-vapor sorption experiments were performed under room temperature and atmospheric pressure. The mole ratio of time-dependent solid-vapor sorption plots was determined by ^{1}H NMR analysis. As shown in Fig. 2a, the adsorption amount of PhH by the activated AdaOH increases with time and finally reaches saturation state after 12 h, while that of Cy by the activated AdaOH is almost negligible. The mole ratio of PhH/AdaOH at the saturated adsorption point is ~0.41. Multi-step TGA result of the saturated AdaOH shows a weight loss of 9.1% from 30 °C to 103 °C after adsorption of PhH vapor for 12 h, also suggesting that one AdaOH molecule can capture 0.41 PhH molecule (Fig. S6 in Supporting information). In contrast, there is no obvious

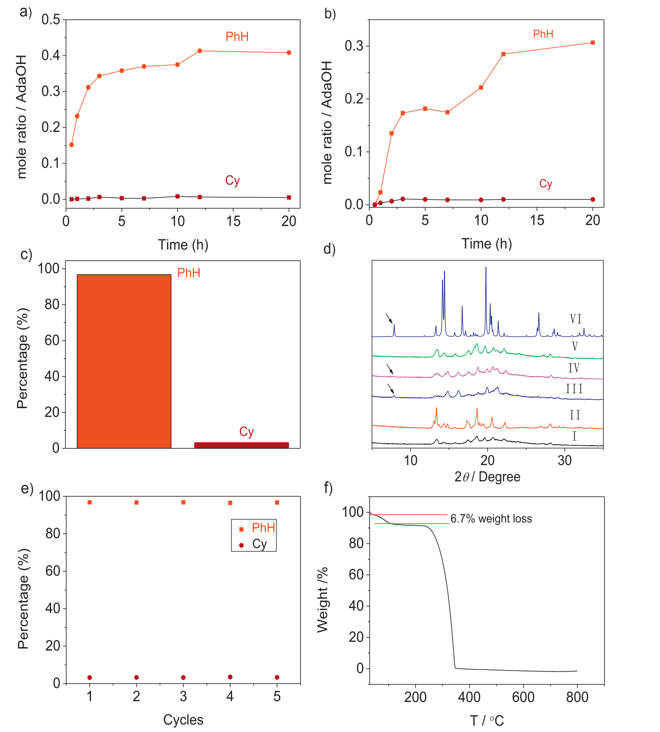

Fig. 2. (a) Time-dependent solid-vapor sorption plots of activated AdaOH for single-component vapors. (b) Time-dependent solid–vapor sorption plot of activated AdaOH for PhH and Cy equal volume mixtures vapor. (c) Relative uptakes of PhH and Cy adsorbed by activated AdaOH that adsorbed PhH/Cy mixtures for 12 h as measured by gas chromatography. (d) PXRD patterns of AdaOH: (I) activated AdaOH; (II) activated AdaOH adsorption of Cy vapour for 12 h; (III) activated AdaOH adsorption of PhH vapour for 12 h; (IV) activated AdaOH adsorption of PhH/Cy mixtures vapour for 12 h; (V) activated AdaOH after adsorption of PhH/Cy mixtures vapour for 12 h and then heating at 150 °C for 2 h; (VI) simulated from single-crystal structure of PhH@$(AdaOH)_2$. (e) Relative uptakes of PhH and Cy by activated AdaOH that adsorbed PhH/Cy mixtures for 12 h after five recycles. (f) Thermogravimetric analysis of activated AdaOH after sorption of PhH/Cy mixtures vapor for 12 h.

weight loss of AdaOH before 200 °C after exposure of the activated of AdaOH to Cy vapor for 12 h. This result indicates that the activated AdaOH cannot capture Cy (Fig. S9 in Supporting information). Moreover, the powder X-ray diffraction (PXRD) patterns of AdaOH after adsorption of PhH vapor for 12 h showed different from the original pattern of activated AdaOH, which implied the structural transformation of activated AdaOH upon capture of PhH vapor (Fig. 2d). In addition, there was no obvious change in PXRD pattern of AdaOH after adsorption of Cy vapor for 12 h (Fig. 2d). These results suggest that the AdaOH shows a high selectivity adsorption capacity for PhH and may be used in the separation of PhH/Cy mixtures. To confirm this hypothesis, two-component (v/v = 1:1) competition solid-vapor sorption experiments were carried out. As shown in Fig. 2b, the adsorption amount of PhH in activated AdaOH was increased with time, while the adsorption of Cy was negligible. After 12 h, one molecule AdaOH could adsorb 0.29 PhH molecules through the ^{1}H NMR and TGA analysis (Fig. 2f and Fig. S10 in Supporting information). This result demonstrates that activated AdaOH has higher selectivity absorption of PhH than Cy. The purity of PhH that adsorbed by activated AdaOH was determined to be 96.8% by gas chromatography analysis (Fig. 2c). Moreover, the reusability property of AdaOH was further tested. The desorption process of PhH is easy to achieve by heating the activated AdaOH at 150 °C for 2 h. ^{1}H NMR spectroscopy, PXRD and TGA analysis suggested the completely released of PhH (Figs. S13–S15 in Supporting information). The re-activated AdaOH solids can be directly re-used for the next adsorption cycle. The AdaOH solid

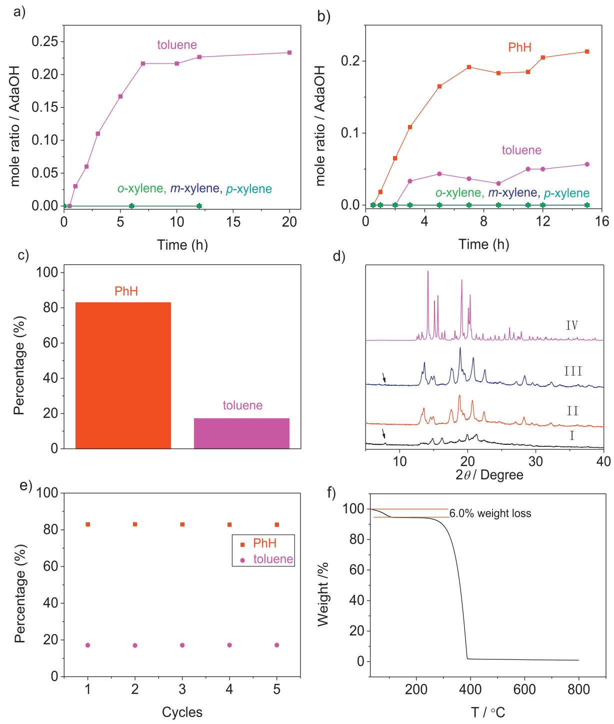

Fig. 3. (a) Time-dependent solid-vapor sorption plots of activated AdaOH for single-component vapors. (b) Time-dependent solid–vapor sorption plot of activated AdaOH for BTX mixtures vapor. (c) Relative uptakes of PhH and toluene adsorbed by activated AdaOH that adsorbed BTX mixtures for 12 h as measured by gas chromatography. (d) PXRD patterns of AdaOH: (I) activated AdaOH adsorption of PhH vapor for 12 h; (II) activated AdaOH adsorption of toluene vapour for 12 h; (III) activated AdaOH adsorption of BTX vapour for 12 h; (IV) simulated from single-crystal structure of toluene@$(AdaOH)_2$. (e) Relative uptakes of PhH and toluene by activated AdaOH that adsorbed BTX mixtures for 12 h after five recycles. (f) Thermogravimetric analysis of activated AdaOH after sorption of BTX mixture vapor for 12 h.

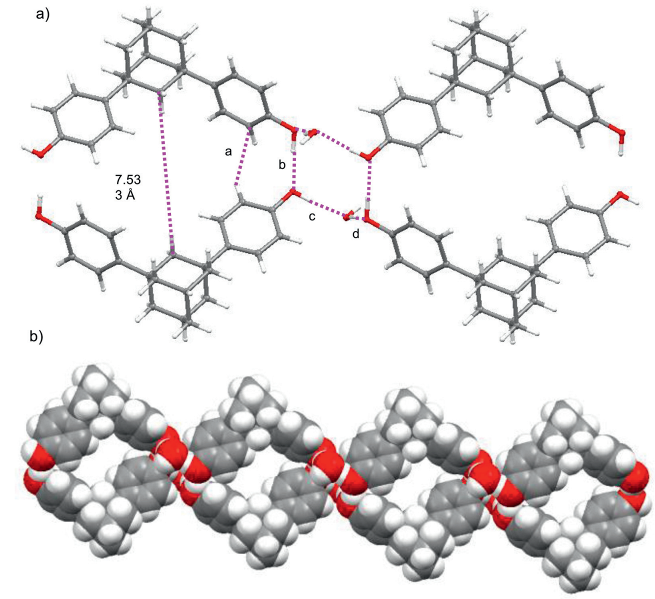

Fig. 4. Crystal structure of AdaOH. (a) The channel-shaped network structure formed by water mediated hydrogen-bonding viewed from the top (along the *a* axis). (b) Space-filling model of the network structure from the front view.

still retained the performance of capturing PhH even after five cycles (Fig. 2e).

Based on these results, we reasoned that the activated AdaOH might be useful for solving the challenge of the separation of BTX mixtures in petrochemical industry. Consequently, single component solid-vapor sorption experiments of activated AdaOH toward toluene, *o*-xylene, *m*-xylene and *p*-xylene were respectively performed under room temperature and atmospheric pressure. As shown in Fig. 3a, the adsorption amount of toluene in activated AdaOH increased with time. The adsorption behavior becomes saturated after ∼12 h. For *o*-xylene, *m*-xylene and *p*-xylenevapors, no adsorption by the activated AdaOH was observed. The saturated activated AdaOH (1 mol) can capture ∼0.23 mol toluene. TGA result showed a weight loss of 6.2% from 30 °C to 127 °C after exposure of the activated AdaOH to toluene vapor for 12 h (Fig. S19 in Supporting information), also confirming the saturated adsorption ratio of 0.23. No obvious weight loss for the TGA profile of the AdaOH ranging from 30 °C to 200 °C was observed after exposure of the activated AdaOH to xylene (v/v, *o*-xylene:*m*-xylene:*p*-xylene = 1:1:1) vapor for 12 h (Fig. S26 in Supporting information). Significantly, the PXRD pattern of activated AdaOH did not change after adsorption of xylene vapor (Fig. S27 in Supporting information) but did change after capture of toluene vapor (Fig. 3d), supporting the absorption of toluene. Inspired by the above results, five-component (v/v; benzene:toluene:*o*-xylene:*m*-xylene:*p*-xylene = 1:1:1:1:1) competition solid-vapor sorption experiments were then carried out. Similar to the single-component solid–vapor sorption experiments, AdaOH does not adsorb *o*-xylene, *m*-xylene and *p*-xylene, but shows a higher selective adsorption of PhH than toluene (Fig. 3b). At the saturated adsorption point (after adsorption for 12 h), the adsorption amount of PhH and toluene were determined as 0.21 PhH and 0.05 toluene molecules per AdaOH from the ^{1}H NMR analysis (Fig. S28 in Supporting information). In addition, the PXRD and TGA analysis of activated AdaOH that adsorbed BTX mixtures further confirming the adsorption of PhH and toluene (Figs. 3d and f). Gas chromatography determined the percentage of PhH adsorbed by activated AdaOH from BTX mixtures to be 82.9% (Fig. S30 in Supporting information), which meant that the purity of PhH was increased from 20% to 82.9%. This result indicates the successful adsorption of PhH from BTX by activated AdaOH. Considering the further real application, the recycling capacity of AdaOH is an important criterion for assessing an adsorbent. Heating the AdaOH that adsorbed BTX at 150 °C for 2 h, the ^{1}H NMR spectroscopy and TGA analysis revealed the completely release of the PhH and toluene from AdaOH (Figs. S31 and S32 in Supporting information). As shown in Fig. 3e, the recycling experiments reveal that no obvious performance loss was observed after five times of AdaOH adsorption ability.

To reveal the mechanism of high adsorption capacity for PhH of activated AdaOH, single crystals of AdaOH, PhH@$(AdaOH)_2$ and toluene@$(AdaOH)_2$ were obtained by slow diffusion of the solution of AdaOH in CH_3CN, CH_3CN/PhH (v:v = 1:1) and CH_3CN/toluene (v:v = 1:1), respectively. However, the single crystals of *o*-xylene@$(AdaOH)_2$, *m*-xylene@$(AdaOH)_2$ and *p*-xylene@$(AdaOH)_2$ cannot be obtained under the same conditions and only obtained the crystals of AdaOH. This may be due to the weak adsorption capacity for xylene of AdaOH, which was consistent with the results before. Similar to the crystal structure of AdaOH in chloroform reported by Tominaga's group [47], the crystal structure of AdaOH grown in CH_3CN can also associated into infinite 1D polymers *via* hydrogen bonds between the hydroxyl groups of phenol parts and water molecules. As shown in Fig. 4a, cyclic structures with sizes of 7.533 Å (measured from the center carbon atom of the adamantane to the center carbon atom of the adamantane) were formed through two molecules of AdaOH by intermolecular hydrogen bonds between the hydroxyl groups of the phenol moieties and water molecules with the distance of 1.826 Å (b), 1.838 Å (c) and 1.853 Å (d), respectively. Moreover, CH···π inter-

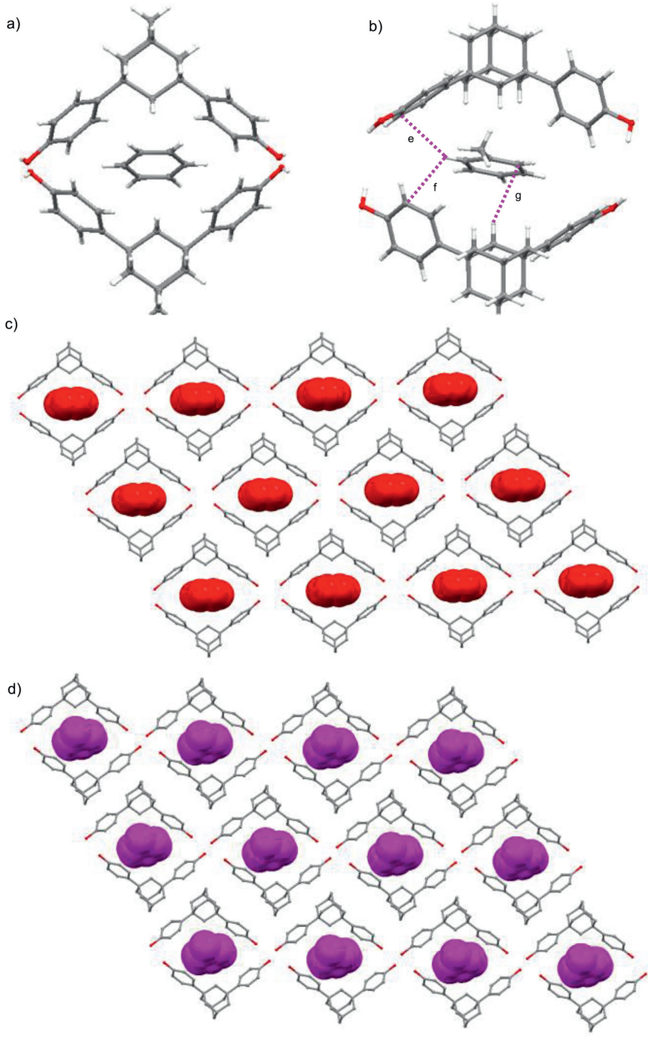

Fig. 5. (a) Crystal structure of PhH@$(AdaOH)_2$. (b) Crystal structure of toluene@$(AdaOH)_2$. (c) Packing structure of PhH@$(AdaOH)_2$, viewed along the *a* axis. (d) Packing structure of toluene@$(AdaOH)_2$, viewed along the *a* axis. Hydrogen atoms are omitted for clarity.

molecular interactions between the phenol moieties with the distance of 2.799 Å (a) were also observed.

We reasoned that the assembly of the AdaOH with cavities might be useful for capturing guest molecules such as PhH and toluene, and the single crystal structures of PhH@$(AdaOH)_2$ and toluene@$(AdaOH)_2$ were thus grown. As expected, in the crystal structure of PhH@$(AdaOH)_2$, PhH molecule was located inside the cavity of the formed cyclic structure by AdaOH to formation of 1:2 complexes. To our surprise, there are no noncovalent interactions between the PhH and AdaOH. The high adsorption capacity of activated AdaOH for PhH may be due to the size matching between the PhH molecule and the formed cyclic structure by AdaOH (Fig. 5a). Similar situation to the structure of PhH@$(AdaOH)_2$, toluene molecule was also located inside the cavity of the formed cyclic structure by AdaOH to formation of 1:2 complexes (Fig. 5b). Additionally, CH$\cdots\pi$ intermolecular interactions between toluene and the phenol moieties of AdaOH with the distance of 2.842 Å (e) and 2.879 Å (f) were observed. It was also found that there were CH$\cdots\pi$ intermolecular interactions between toluene and the adamantane moieties of AdaOH with the distance of 2.887 Å (g). Because of these multi noncovalent interactions, the toluene molecules were firmly embedded in the cavity of the formed cyclic structure by AdaOH. From the a-axis direction of PhH@$(AdaOH)_2$ and toluene@$(AdaOH)_2$ complex packing structure, a large number of PhH and toluene molecules are captured in the crystal structure.

In summary, we reported the use of commercially available AdaOH as a non-porous adaptive crystal to separate PhH from mixed vapors of Cy and BTX under conditions of room temperature and atmospheric pressure for the first time. We attribute the high selective capturing performance of AdaOH toward PhH to the formation of an infinite 1D assembly of AdaOH with cavities that are well-suited for the capturing PhH. The purity of PhH, that are separated from a mixture of equimolar PhH and Cy by using the avtivated AdaOH, was as high as 96.8%. When using the activated AdaOH to separate PhH from BTX vapor, the purity of PhH can be as high as 82.9%. The new discovery of using the activated AdaOH as a non-porous adaptive crystal for selectively and efficiently capturing PhH can solve the challenge in separation of benzene from other chemicals such as Cy in chemical industry, and can be helpful for removal of benzene that is released from the vehicles to air. The advantages of commercially availability, easy preparation, high separation efficiency and selectivity for benzene, and excellent recycling performance of the AdaOH endow this material with enormous potential for uses in the petrochemical industry. We will further focus on developing AdaOH derivatives to improve the performance for separating PhH from BTX vapor.

Declaration of competing interest

The authors declare that they have no known competing financial interests or personal relationships that could have appeared to influence the work reported in this paper.

Acknowledgments

The authors are grateful for the financial support from the National Natural Science Foundation of China (No. 21602055); Natural Science Foundation of Hunan Province (No. 2017JJ3094).

Supplementary materials

Supplementary material associated with this article can be found, in the online version, at doi:10.1016/j.cclet.2023.108304.

References

[1] S.M. Correa, G. Arbilla, M.R.C. Marques, et al., Atmos. Pollut. Res. 3 (2012) 163–169.
[2] A. Salvi, G. Patki, H. Liu, et al., Sci. Rep. 7 (2017) 8306.
[3] BenzeneAir Quality Guidelines For Europe, 2nd ed., World Health Organization, Copenhagen, 2000.
[4] B. Szala, T. Bajda, J. Matusik, et al., Micropor. Mesopor. Mater. 202 (2015) 115–123.
[5] D.M. Ruthven, Principles of Adsorption and Adsorption Processes, 3rd ed., John Wiley & Sons, Inc., New York, 1984.
[6] A.A. Daifullah, B. Girgis, Coll. Surf. A Physicochem. Eng. Asp. 214 (2003) 181–193.
[7] Y. Li, G. Gupta, J. Hazard. Mater. 38 (1994) 105–112.
[8] M.S. Paula, V. Alexsandra, M.A.G. de US Selene, et al., Fuel 231 (2018) 45–52.
[9] A. Prabhu, A. Al. Shoaibi, C. Srinivasakannan, Appl. Catal. A Gen. 466 (2013) 137–141.
[10] S. Shimomura, S. Horike, R. Matsuda, et al., J. Am. Chem. Soc. 129 (2007) 10990–10991.
[11] X. Wang, Y. Wang, K. Lu, et al., Chin. Chem. Lett. 32 (2021) 1169–1172.
[12] Y.L. X, Q. Gao, M. Zhao, et al., Chin. Chem. Lett. 28 (2017) 55–59.
[13] R. Yang, L. Li, Y. Xiong, et al., Chem. Asian J. 5 (2010) 2358–2368.
[14] S. Mukherjee, D. Sensharma, O.T. Qazvini, et al., Coord. Chem. Rev. 437 (2021) 213852.
[15] L. Yang, C. Shi, L. Li, et al., Chin. Chem. Lett. 31 (2020) 227–230.
[16] L.K. Macreadie, E.J. Mensforth, R. Babarao, et al., J. Am. Chem. Soc. 141 (2019) 3828–3832.
[17] J. Li, Y. He, Y. Zou, et al., Chin. Chem. Lett. 33 (2022) 3017–3020.
[18] L. Li, R. Lin, X. Wang, et al., Chem. Eng. J. 354 (2018) 977–982.
[19] A. Cadiau, K. Adil, P.M. Bhatt, et al., Science 353 (2016) 137–140.
[20] J. Hou, L. Liu, Y. Li, et al., Environ. Sci. Technol. 47 (2013) 13730–13736.

[21] A. Stanislaus, B.H. Cooper, Catal. Rev. Sci. Eng. 36 (1994) 75–123.
[22] D.S. Sholl, R.P. Lively, Nature 532 (2016) 435–437.
[23] T. Ogoshi, Y. Shimada, Y. Sakata, et al., J. Am. Chem. Soc. 139 (2017) 5664–5667.
[24] J.R. Wu, Y.W. Yang, J. Am. Chem. Soc. 141 (2019) 12280–12287.
[25] J.R. Wu, Y.W. Yang, CCS Chem. 2 (2020) 836–843.
[26] J.R. Wu, B. Li, Y.W. Yang, Angew. Chem. Int. Ed. 59 (2020) 2251–2255.
[27] Y. Wang, K. Xu, B. Li, Angew. Chem. Int. Ed. 58 (2019) 10281–10284.
[28] H.Y. Zhou, C.F. Chen, Chem. Commun. 58 (2022) 4356–4359.
[29] Y. Zhou, K. Jie, E. Li, et al., Sci. Sin. Chim. 49 (2019) 832–843.
[30] M. Wang, J. Zhou, E. Li, et al., J. Am. Chem. Soc. 141 (2019) 17102–17106.
[31] K. Jie, M. Liu, Y. Zhou, et al., J. Am. Chem. Soc. 139 (2017) 2908–2911.
[32] K. Jie, Y. Zhou, E. Li, et al., J. Am. Chem. Soc. 140 (2018) 3190–3193.
[33] Y. Zhao, H. Xiao, C.H. Tung, et al., Chem. Sci. 12 (2021) 15528–15532.
[34] S. Niu, L.L. Mao, H. Xiao, et al., Chin. Chem. Lett. 33 (2022) 1970–1974.
[35] D. Luo, J. Tian, J.L. Sessler, et al., J. Am. Chem. Soc. 143 (2021) 18849–18853.
[36] Q. Li, K. Jie, F. Huang, Angew. Chem. Int. Ed. 59 (2020) 5355–5358.
[37] T. Xiao, L. Zhou, X.Q. Sun, et al., Chin. Chem. Lett. 31 (2020) 1–9.
[38] J. Zhou, G. Yu, Q. Li, et al., J. Am. Chem. Soc. 142 (2020) 2228–2232.
[39] W. Yang, K. Samanta, X. Wan, et al., Angew. Chem. Int. Ed. 59 (2020) 3994–3999.
[40] H. Yao, Y.M. Wang, M. Quan, et al., Angew. Chem. Int. Ed. 59 (2020) 19945–19950.
[41] Y. Ding, O.A. L.ukman, M. Basem, et al., Chem. Sci. 12 (2021) 5315–5318.
[42] F. Zeng, L. Cheng, W.J. Zhang, et al., Org. Chem. Front. 9 (2022) 3307–3311.
[43] R. Sumida, T. Matsumoto, T. Yokoi, et al., Chem. Eur. J. (2022) e202202825.
[44] F. Zeng, X.S. Xiao, S.F. Gong, et al., Org. Chem. Front. 9 (2022) 4829–4833.
[45] Y. Hou, Y.R. Duan, M.H. Ding, et al., RSC Adv. 12 (2022) 22060–22063.
[46] M.H. Ding, J. Liao, L.L. Tang, et al., Chin. Chem. Lett. 32 (2021) 1665–1668.
[47] M. Tominaga, H. Masu, I. Azumaya, Cryst. Growth Des. 11 (2011) 542–546.